Saudi Journal of Biological Sciences 24 (2017) 1866–1870

Contents lists available at ScienceDirect

Saudi Journal of Biological Sciences

journal homepage: www.sciencedirect.com

Original article

Rock signaling control PPARγ expression and actin polymerization during adipogenesis

Yuntao Ji [1], Meixia Cao [1], Jia Liu, Yanfei Chen, Xiaoli Li, Jing Zhao, Changqing Qu *

School of Biology and Food Engineering, FuYang Normal University, Fuyang, Anhui 236041, China

ARTICLE INFO

Article history:
Received 30 September 2017
Revised 9 November 2017
Accepted 9 November 2017
Available online 11 November 2017

Keywords:
C3H10T1/2
RhoA/ROCK
Adipogenesis
PPARγ
Actin polymerization

ABSTRACT

Aim: Adipogenesis is characterized by a strong interdependence between cell shape, cytoskeletal organization, and the onset of adipogenic gene expression. Here we investigated the role of the RhoA/ROCK pathway in adipogenesis. *Result:* High RhoA activity in the cell line C3H10T1/2 were generated (Named RhoA14V cells). Treatment of RhoA14V cells with Shield 1 following their differentiation into adipocytes resulted in the appearance of thick cortical actin filaments, and increased mRNA expression levels of RhoA, ROCK, p-MYPT1 and p-MLC, while PPARγ mRNA decreased. This resulted in decreased triglyceride synthesis and reduced expression of the adipogenic transcription factor PPARγ. These molecular changes were accompanied by reorganization of the actin cytoskeleton, during which ROCK signaling suppressed actin polymerization. *Conclusion:* ROCK signaling suppresses adipogenesis by controlling PPARγ expression and actin organization in adipocytes.

1. Introduction

Adipose tissue is a reservoir of fat that functions as the main form of energy storage (Ruan et al., 2014). In the past decade, adipose tissue and adipocytes have become a global focus of research (Kavalkova et al., 2013) Too little body fat caused by deficient fat uptake can lead to severe metabolic disorders, such as hypertriglyceridemia and early onset type II diabetes mellitus. However, fat accumulation causes obesity, which increases the risk of cardiovascular diseases, type II diabetes and metabolic syndrome (Fox, 2008).

Rho is a member of the Ras sub-family of the small GTPase super-family. Since the first report by Pascal Madaule in 1985, over 20 Rho family proteins have been discovered (Ridley, 2001). Rho family proteins are 20–25 kDa GTP-bound proteins with GTPase activity. These proteins are bound to GTP in the active state, and to GDP in the inactive state. Rho proteins regulate downstream signaling molecules by switching between these two state (Wennerberg and Der, 2004). By regulating the Rho kinase, ROCK, and its downstream proteins, MYPT and MLC, Rho regulates depolarization of the actin skeleton, which modulates cellular polarity and morphology, as well as adipogenesis. Rho proteins can be categorized into RhoA, Racl, Cdc24 and non-GTPase sub-families according to the degree of homology and function. Activation of RhoA is required for actin-based cytoskeletal contraction. G14V or Q63L mutations cause Rho to persist in the activated GTP-bound state due to impaired hydrolysis (Mack et al., 2001), thus enhancing the function of the mutant form. In this study, we investigated the role of Rho and RhoA/ROCK signaling in adipogenesis by overexpressing RhoA14V and inducing adipogenic differentiation in stable expression clones. Our results may provide a theoretical basis for modulation of body fat deposition and reveal a potential therapeutic target for obesity-related diseases.

2. Material and methods

2.1. Cell strains and cell culture

C3H10T1/2 was obtained from the Institute of Biochemistry and Cell Biology, SIBS, CAS (Shanghai, China). The C3H10T1/2 cells were maintained in DMEM medium (Hyclone, USA) supplemented with 10% fetal bovine serum (FBS; Hyclone) and cultured under a humidified atmosphere of 5% CO_2 and 95% air at 37 °C. The Plat-E Retrovirus Packaging cell line was obtained from the Cell Biolabs. Plat-E cells were maintained in DMEM supplemented with 10%

* Corresponding author.
E-mail address: qucq518@163.com (C. Qu).
[1] Co-author.
Peer review under responsibility of King Saud University.

Production and hosting by Elsevier

https://doi.org/10.1016/j.sjbs.2017.11.029
1319-562X/

FBS) and containing 1 μg/mL puromycin, 10 μg/mL blasticidin, penicillin and streptomycin and cultured under a humidified atmosphere of 5% CO_2 and 95% air at 37 °C. C3H10T1/2 cells were grown to confluence and induced to differentiate into adipocytes by exposure to a cocktail containing DMEM supplemented with 10% FBS, 0.5 mM IBMX (Sigma, USA), 0.1 mM dexamethasone (Sigma), and 0.2 mg/L insulin and 0.5 mM rosiglitazone (Sigma) for 48 h. Subsequently, the cells were switched to differentiation medium (DMEM, 10% FBS, 0.1 mM dexamethasone (Sigma), and 0.2 mg/L insulin for 48 h. Cells were then cultured 4 or 8 days in DMEM with 10% FBS.

2.2. Oil-Red O staining and lipid quantification

At 4 or 8 days after differentiation treatment, removed the cells and treated with 4% paraformaldehyde for 35 min at RT. Cells were washed three times in phosphate buffered saline (PBS) and incubated with oil-red O working solution (0.5% oil-red O in isopropanol: deionized water mixed at 3:2 immediately before use) for 40 min. The cells were then washed with PBS and lipid droplets stained with oil-red O were extracted in 200 μL of absolute isopropyl alcohol for quantification by measuring the absorbance at 490 nm. Triglyceride levels were measured using a triglyceride (TG) assay kit according to the manufacturer's instructions. The TG assays were repeated in triplicate.

2.3. PCR method

Total RNA from C3H10T1/2 and RhoA14V cells was extracted using TRIzol reagent according to the manufacturer's instructions (Invitrogen). Reverse transcription-PCR (RT-PCR) was performed using Fermentas K1622 RevertAid™ First Strand cDNA Synthesis Kit (Fermentas). RT-qPCR was performed with a SYBR PrimeScript™ RT-PCR kit (TaKaRa) using the ABI PRISM 7500 Real-Time PCR System (Applied Biosystems, Foster City, CA, USA). The sequence specific primers are showed in Table 1. The relative gene expression of each sample was shown.

2.4. Western blot

C3H10T1/2 cells were cultured on 60-mm plates for different periods of time, suspended and lysed in 200 μL lysis buffer containing a complete protease inhibitor cocktail and PhosStop (Roche, USA) for 30 min on ice. The lysates were centrifugated at 12,000 rpm for 5 min at 4 °C. Protein concentrations were quantified by the BCA protein assay kit (Beyotime, Shanghai, China), boiled 5 min mixed with a sample loading buffer before separation by SDS-PAGE. The proteins were then electro- transferred to polyvinylidene difluoride (PVDF) membranes (Millipore, Bedford, MA, USA), blocked by incubation with 5% non-fat milk for 1 h and incubated with the primary antibodies for the detection of RhoA (67B9), ROCK2 (D1B1), MYPT1 (2364) (diluted 1:1,000; Cell Signaling Technology, Danvers, MA, USA); MLC (ab92721) P-MLC (ab2480) (diluted 1:5,000; Abcam); and GAPDH (diluted 1:500; Goodhere Biotechnology, Hangzhou, China) overnight at 4 °C. After washing, the membranes were then incubated with specific horseradish peroxidase-conjugated secondary antibodies and visualized using an electrochemiluminescence reagent.

Table 1
Primer sequences used in RT-**q**PCR.

Genes	Primers
PPARγ	S:5′-TGTCTCACAATGCCATCAGGTT-3′ A:5′-TGGTGATTTGTCCGTTGTCTTTC-3′
C/EBPα	S:5′-CAGAGGGACTGGAGTTATGACAAG-3′ A:5′-CCCAGCCGTTAGTGAAGAGTC-3′
RhoA	S:5′-GGATGGGAAGCAGGTAGAGTTG-3′ A:5′-CGGCTCCTGCTTCATTTTGG-3′
β-actin	S: 5′-CAGCCTTCCTTCTTGGGTATGG-3′ A:5′-TGTGTTGGCATAGAGGTCTTTACG-3′

2.5. Statistical analysis

All data are presented as the means ± SD and were analyzed by the SPSS 22.0 software package. Differences between groups were examined for statistical significance using unpaired Student's *t*-tests. Multiple comparisons were analyzed by one-way ANOVA. $P < .05$ was considered to indicate statistical significance.

3. Results and discussion

3.1. Lipid quantification by oil-red O staining

RhoA14V and control C3H10T1/2 cells following the induction of adipogenic differentiation stained by oil red O. The number of red-stained lipid droplets increased with time during the process of adipogenic differentiation in both RhoA14V and C3H10T1/2 cells. Furthermore, the cell morphology changed from the original fibroblast-like appearance to an irregular shape and finally, to oval in the late stage of differentiation. Notably, there were fewer lipid droplets with smaller volumes in the RhoA14V cells than in the control C3H10T1/2 cells. At 4 d, numerous lipid droplets were visible in the cytoplasm of C3H10T1/2 cells, while only tiny lipid droplets were observed in some of the RhoA14V cells. At 8 d, the lipid droplets in the control C3H10T1/2 cells became were larger and more numerous, and they formed a circle surrounding the nucleus (Fig. 1).

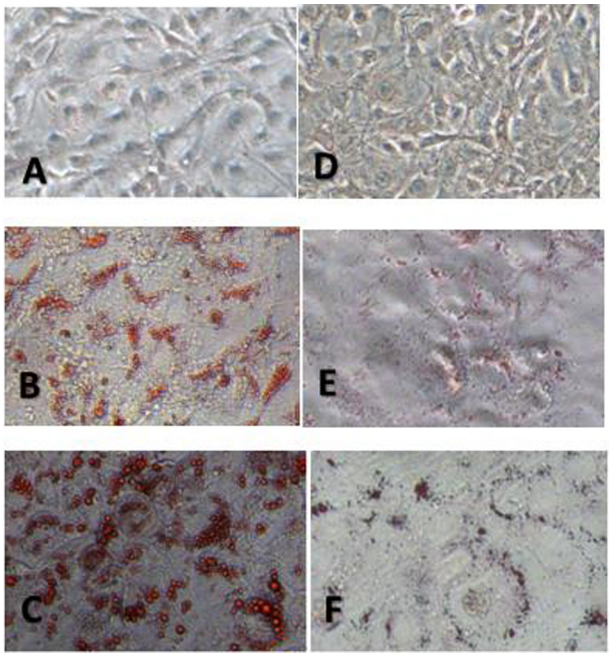

Fig. 1. Oil-red O staining of C3H10T1/2 cells at different time-points after the induction of adipogenic differentiation (oil-red O staining, 200×). A: Confluent C3H10T1/2 cells on day 0 (200×); B: C3H10T1/2 cells stained with oil-red O on day 4 (200×); C: C3H10T1/2 cells stained with oil-red O at 8 d (200×); D: Confluent RhoA14V cells at 0 d (200×); E: RhoA14V cells stained with oil-red O at 4 d (200×); F: RhoA14V cells stained with oil-red O at 8 d (200×).

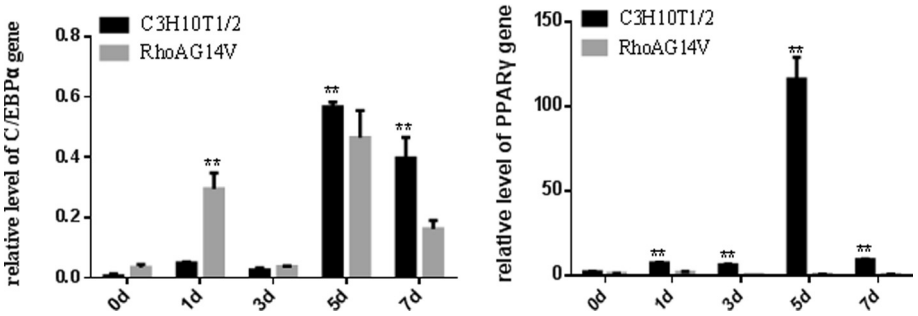

Fig. 2. Changes in C/EBPα and PPARγ gene expression during adipogenic differentiation. $^{*}P < .05$; $^{**}P < .01$ compared with control C3H10T1/2 cells.

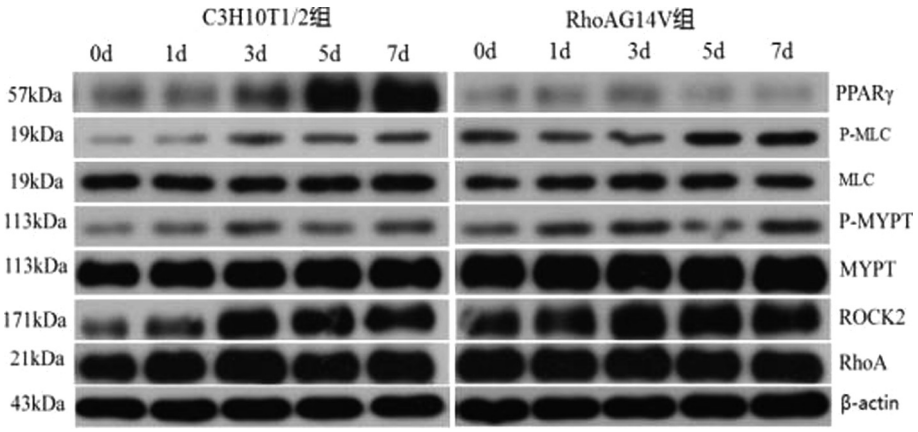

Fig. 3. Western blot detection of changes in the expression of proteins during adipogenic differentiation. $^{*}P < .05$; $^{**}P < .01$ compared with control C3H10T1/2 cells.

3.2. Effect of RhoA14V on adipogenic gene expression

The pattern of changes in C/EBPα gene expression during adipogenic differentiation was similar in control C3H10T1/2 and RhoA14V cells. Specifically, peak expression occurred at 1 d and 5 d after the induction of differentiation, with maximum expression reached at 5 d. While PPARγ expression in control C3H10T1/2 cells first increased and then declined during the course of adipogenic differentiation, with maximal expression observed at 5 d. In contrast, PPARγ expression decreased gradually in RhoA14V cells during adipogenic differentiation. PPARγ expression levels were higher in the control cells than those in the RhoA14V cells throughout the differentiation process (Fig. 2).

3.3. Effects of RhoA14V on the expression of key genes in the ROCK signaling pathway in C3H10T1/2 cells

The changes in expression of RhoA, ROCK, MYPT1, p-MYPT1, MLC, p-MLC and PPARγ proteins in RhoA14V cells and control C3H10T1/2 cells were analyzed during adipogenic differentiation. Western blotting showed that RhoA expression declined gradually during adipogenic differentiation in both RhoA14V and control C3H10T1/2 cells (Fig. 3).

RhoA expression levels were higher in RhoA14V cells than those in control C3H10T1/2 cells at all the time-points investigated during the differentiation process, with significant differences detected at 0 h, 1 h and 7 d ($P < .05$). The expression levels of ROCK, MYPT1 and p-MYPT1 were relatively stable in RhoA14V cells, whereas ROCK expression first increased and then decreased in control C3H10T1/2 cells. ROCK expression levels were higher in RhoA14V cells than those in control C3H10T1/2 cells during the process of differentiation except at 3 d, with significant differences detected at 0 d, 1 d and 5 d ($P < .05$). In control C3H10T1/2 cells, MLC expression levels increased initially, followed by a decline and then a recurrence of the increased expression, while p-MLC levels first increased and then decreased, with the maximal level detected at 3 d. In RhoA14V cells, the levels of MYPT1 and p-MYPT1 gradually increased during adipogenic differentiation. The level of p-MLC was higher in RhoA14V cells than that in control C3H10T1/2 cells at all time-points investigated during the differentiation process, with significant differences detected at 0 d, 1 d, 5 d and 7 d ($P < .05$). During adipogenic differentiation, PPARγ expression declined in RhoA14V cells, while the levels increased in control C3H10T1/2 cells. PPARγ expression was lower in RhoA14V cells than that in the control cells at all time-points investigated throughout the differentiation process, with significant differences detected at 5 d and 7 d ($P < .05$).

3.4. Cytoskeletal morphology in RhoA14V cells during adipogenic differentiation

Microscopic observation showed that the control cells were spindle-formed, and actin filaments surrounding the nucleus exhibited green fluorescence and were in reticular arrangement, with clearly visible stress fibers at the cell periphery. The RhoA14V cells showed concentric retraction with filopodia and lamellar pseudopodia formed at the periphery. Cytoskeletal relaxation was observed gradually during adipogenic differentiation in both RhoA14V cells control C3H10T1/2 cells. The regular arrangement of actin filaments in the control cells disappeared, and the cytoskeleton was depolymerized. The filopodia and lamellar pseudopodia were slightly unfolded in some of the RhoA14V cells, while filament polymerization around the nucleus was observed in other RhoA14V cells (Fig. 4).

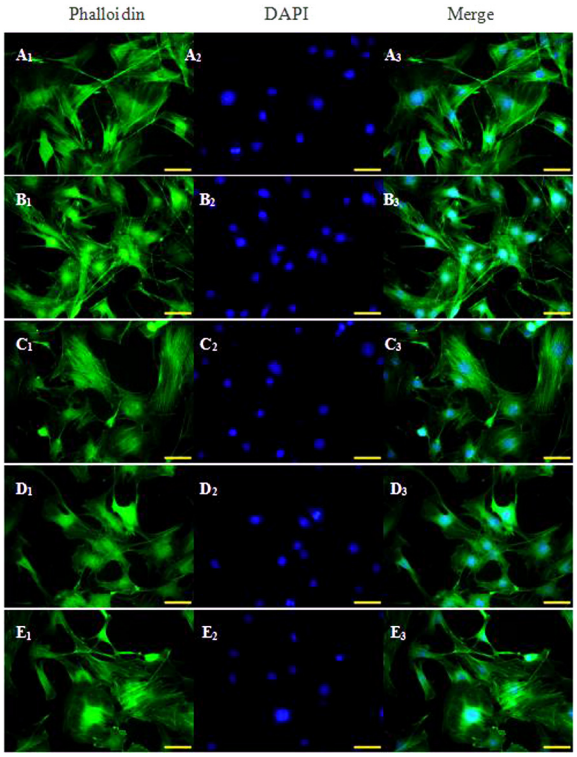

Fig. 4. Laser scanning confocal microscopy images of rhodamine-phalloidin-stained cytoskeleton in RhoA14V cells during adipogenic differentiation. A_1–A_3: 0 d; B_1–B_3: 1 d; C_1–C_3: 3 d; D_1–D_3: 5 d; E_1–E_3: 7 d.

4. Conclusions

Our study established a C3H10T1/2 cell line with stable overexpression of RhoA as a reliable cell model for the subsequent studies. In the presence of adipogenic factors, cultured C3H10T1/2 cells are directed to differentiate into adipocytes precursor cells (APCs), then preadipocytes, and finally mature adipocytes through the processes of mitotic division and terminal differentiation. A number of transcription factors are known to play key roles in differentiation process, such as PPARγ, C/EBPs and SREBPs. RT-qPCR analysis of RhoA14Vcells at 0 d, 1 d, 3 d, 5 d, and 7 d after the induction of adipogenic differentiation imply that RhoA14V reduced the potency of adipogenic differentiation in C3H10T1/2 cells, probably by inhibiting the expression of the key adipogenic gene, PPARγ. Kusuyama et al. (2014) found that low-intensity pulsed ultrasound (LIPUS) stimulation of multi-lineage MSC differentiation reduced the expression of PPARγ through activation of ROCK, thereby inhibiting adipogenic differentiation. Moreover, the effect of LIPUS on cell differentiation was abolished in the presence of a ROCK inhibitor, Y-27632. Yu et al. (2012). reported that C/EBPα expression was reduced when PPARγ was silenced during adipogenic differentiation. In addition, Xu et al. (2012) demonstrated a role of RhoA/ROCKII in fate determination during MSC differentiation. Inhibition of RhoA or ROCKII promoted the commitment of MSCs to adipocytes or cartilage, whereas activation of RhoA or ROCKII induced differentiation into osteoblasts. Western blot analysis of the changes in the expression of RhoA, ROCK, MYPT1, p-MYPT1, MLC, p-MLC and PPARγ proteins in RhoA14V and control cells during adipogenic process indicated that RhoA14V upregulated the expression of MYPT and MLC, which are downstream molecules in the RhoA/ROCK signaling pathway, and also reduced the expression of the adipogenic marker, PPARγ. Arnsdorf et al. (2009) demonstrated modulation of multiple transcription factors and cell fate determination in C3H10T1/2 cells by flow shear forces. The differentiation of C3H10T1/2 cells in response to the shear force generated by fluid flow was investigated in a parallel-plane flow chamber that mimicked the physiological environment *in vivo*. The fluid flow increased the expression of the adipogenic PPARγ, while activation of RhoA and its downstream effector protein ROCK downregulated PPARγ expression, resulting in overall inhibition of adipogenic or chondrogenic differentiation. In addition, Nuttall and Gimble (2004) demonstrated that PPARγ promoted adipogenic differentiation, but inhibited osteogenic differentiation in bone marrow MSCs. Megakaryoblastic leukemia-1 (MKL1), which is universally expressed in living organisms, couples with G-actin monomer in the cytoplasm to form complexes that antagonize PPARγ-mediated regulation of adipogenesis. At high cellular MKL1 levels, G-actin uncouples, leading to increased F-actin expression, cytoskeletal polymerization, and PPARγ downregulation, which ultimately reduces the adipogenic potential of the cells (Nobusue et al., 2014).

Fluorescence microscopy revealed spindle-shaped morphology of the control C3H10T1/2 cells, with green fluorescent actin filaments surrounding the nucleus in a reticular arrangement. In contrast, RhoA14V cells showed concentric retraction with filopodia and lamellar pseudopodia formed at the periphery. The cytoskeleton gradually relaxed in both RhoA14V cells and control C3H10T1/2 cells during adipogenic differentiation. Furthermore, the regular arrangement of actin filaments in the control cells disappeared, while slight unfolding of the filopodia and lamellar pseudopodia in the RhoA14V cells occurred. Our data suggest that actin polymerization and reduction in G-actin in response to RhoA-overexpression leads to a rise in intracellular MKL1 levels, which represses PPARγ expression and results in reduced adipogenic potential in the cell.

Acknowledgements

This research was financially supported by grants from the National Natural Science Foundation of China (No. 31201788, No. 31172182) and Innovation team project of Anhui Scientific research platform (2016) and National Undergraduate Training Programs for Innovation and Entrepreneurship (201510371062, 201510371065, 201510371068, 201510371019, 201510371020).

References

Arnsdorf, E.J., Tummala, P., Kwon, R.Y., et al., 2009. Mechanically induced osteogenic differentiation -the role of RhoA, ROCKII and cytoskeletal dynamics. J. Cell Sci. 122, 546–553.

Fox, E.M., 2008. Estrogen Receptor Alpha and STAT5b Crosstalk: Implications for Estrogen-stimulated Breast Cancer Proliferation. ProQuest.

Kavalkova, P., Touskova, V., Roubicek, T., et al., 2013. Serum preadipocyte factor-1 concentrations in females with obesity and type 2 diabetes mellitus: the influence of very low calorie diet, acute hyperinsulinemia, and fenofibrate treatment. Horm Metab Res. 45, 820–826.

Kusuyama, J., Bandow, K., Shamoto, M., et al., 2014. Low-Intensity Pulsed Ultrasound (LIPUS) Influences the multi-lineage differentiation of mesenchymal stem and progenitor cell lines through ROCK-Cot/Tpl2-MEK-ERK signaling pathway. J. Cell Biol. 289, 10330–10344.

Mack, C.P., Somlyo, A.V., Hautmann, M., et al., 2001. Smooth muscle differentiation marker gene expression is regulated by RhoA-mediated actin polymerization. J. Biol. Chem. 276, 341–347.

Nobusue, H., Onishi, N., Shimizu, T., et al., 2014. Regulation of MKL1 via actin cytoskeleton dynamics drives adipocyte differentiation. Nat. Commun. 5, 3368.

Nuttall, M.E., Gimble, J.M., 2004. Controlling the balance between osteoblastogenesis and adipogenesis and the consequent therapeutic implications. Curr. Opin. Pharmacol. 4, 290–294.

Ridley, A.J., 2001. Rho family proteins: coordinating cell responses. Trends Cell Biol. 11, 471–477.

Ruan, H.B., Dietrich, M.O., Liu, Z.W., et al., 2014. O-GlcNAc transferase enables AgRP neurons to suppress browning of white fat. Cell. 159, 306–317.

Wennerberg, K., Der, C.J., 2004. Rho-family GTPases: it's not only Rac and Rho. J. Cell Sci. 117, 1301–1312.

Xu, T., Wu, M., Feng, J., et al., 2012. RhoA/Rho kinase signaling regulates transforming growth factor-β1-induced chondrogenesis and actin organization of synovium-derived mesenchymal stem cells through interaction with the Smad pathway. Int. J. Mol. Med. 30, 11–19.

Yu, W.H., Li, F.G., Chen, X.Y., et al., 2012. PPARγ suppression inhibits adipogenesis but does not promote osteogenesis of human mesenchymal stem cells. Int. J. Biochem. Cell Biol. 44, 377–384.